Dual-Branch MRC Receivers in the Cellular Downlink under Spatial Interference Correlation

Ralph Tanbourgi*, Harpreet S. Dhillon†, Jeffrey G. Andrews‡ and Friedrich K. Jondral*

***Abstract*—Although maximal-ratio combining (MRC) has become a widespread diversity-combining technique, its performance under interference is still not very well understood. Since the interference received at each antenna originates from the same set of interferers, but partially de-correlates over the fading channel, it exhibits a complicated correlation structure across antennas. Using tools from stochastic geometry, this work develops a realistic analysis capturing the interference correlation effects for dual-branch MRC receivers in a downlink cellular system. Modeling the base station locations by a Poisson point process, the probability of a typical dual-branch MRC receiver being covered by its serving base station is derived. For the interference-limited case, this result can be further simplified to an easy-to-use single-integral expression. Using this result, it is shown that ignoring interference correlation overestimates the true performance by 3%–10%, while assuming identical interference levels across antennas underestimates it by <2%. In both cases, however, the true diversity order of dual-branch MRC is preserved. Finally, the performance of MRC and selection combining under spatial interference correlation is compared.**

***Index Terms*—Multi-antenna receivers, maximal-ratio combining, interference correlation, Poisson point process.**

I. Introduction

Maximal-ratio combining (MRC) is a ubiquitous diversity combining technique for modern multi-antenna devices such as smartphones, laptops, or, more recently, vehicular-integrated communications systems. It is tailored to combating the effects of channel fading in order to improve link reliability. Like other diversity combining schemes, MRC suffers performance losses when non-idealities such as average reception-quality imbalance [1] and correlation across antennas [2] are considered. These performance losses become more severe when (multi-user) interference—typically being the performance-limiting factor in cellular networks—is taken into account. This is because interference is usually not equally strong across antennas since the interferer to per-antenna links undergo un/slightly-correlated fading as well; thereby further increasing reception-quality imbalance across antennas [3]. Moreover, this imbalance is usually highly dynamic and entails a complicated correlation structure across antennas that depends upon various system parameters including the locations of interferers. More specifically, the interference seen at each antenna originates from the *same* set of interferers, but *partially de-correlates* over the fading channel; making a tractable analysis difficult. A promising way to capture such complex interference effects, while maintaining tractability, is to use tools from *stochastic geometry* [4], [5]. Along several works in this domain studying the effects of interference correlation [6]–[10], the performance of multi-antenna MRC receivers under spatially-correlated interference in decentralized networks was recently characterized in [11], [12]. These works in particular showed that assuming a simple interference correlation model—as frequently done in the literature—may considerably distort the performance prediction of MRC under correlated interference. More specifically, when ignoring interference correlation, i.e., assuming that interferers originate from distinct sets for each antenna [13], the true performance is significantly overestimated. Conversely, assuming identical interference levels across antennas, as done for instance in [14], underestimates the true performance of MRC.

In this paper, we consider a downlink cellular system where dual-antenna receivers employ MRC. Compared to [11], [12], such an extension to the cellular case is non-trivial since the interference/reception properties substantially differ from the case of decentralized networks due to the cell-association mechanism in cellular networks. Note that the dual-antenna case is of particular interest in view of the space and complexity limitations of practical downlink receivers. Our contributions are summarized below.

Analytical model and coverage probability: We develop a tractable model for characterizing the cellular downlink performance of dual-antenna MRC receivers. The model accounts for irregular base station (BS) deployments and relevant system parameters such as BS density, path loss, fading and receiver noise. As the key result, we derive the coverage probability (cf. Definition 1) for a typical dual-antenna MRC receiver. In the interference-limited case, this result reduces to an easy-to-use single-integral expression.

Comparison with simpler correlation models: Using the key result, we analyze the coverage probability gap when employing popular though simpler correlation models. It is found that ignoring interference correlation across antennas yields a 3%–10% higher coverage probability for typical path loss exponents. In contrast, assuming identical interference levels across antennas underestimates the true coverage probability by no more than 2%. This observation thus justifies the use of the popular full-correlation model in cellular network analysis.

*R. Tanbourgi and F. K. Jondral are with the Communications Engineering Lab (CEL), Karlsruhe Institute of Technology (KIT), Germany. Email: {ralph.tanbourgi, friedrich.jondral}@kit.edu. This work was partially supported by the German Research Foundation (DFG) within the Priority Program 1397 "COIN" under grant No. JO258/21-2.

†H. S. Dhillon is with the Communication Sciences Institute (CSI), Department of Electrical Engineering, University of Southern California, Los Angeles, CA. Email: hdhillon@usc.edu.

‡J. G. Andrews is with the Wireless and Networking Communications Group (WNCG), The University of Texas at Austin, TX, USA. Email: jandrews@ece.utexas.edu.

Design insights for dual-branch MRC: The coverage probability gain over single-antenna receivers monotonically increases with the target spectral efficiency, and monotonically decreases with the path loss exponent. For typical operating points, the improvement ranges from 12% to 67%. The diversity order remains unaffected by interference correlation and its value is preserved by the two simpler correlation models discussed in this work. Under spatial interference correlation, MRC offers a coverage probability gain over selection combining (SC) of roughly 20% at small path loss exponents. For large path loss exponents, the higher complexity of MRC may not be justified as SC exhibits similar performance.

Notation: We use sans-serif-style letters (z) for denoting random variables and serif-style letters (z) for denoting their realizations or variables. We define $(z)^+ \triangleq \max\{0, z\}$.

II. System Model

We consider a co-channel cellular network in the downlink. To account for irregular BS deployments typically encountered in practice, we model the locations x_i of BSs by a stationary planar Poisson point process (PPP) Φ with density λ [BSs/m^2], i.e., $\{\mathsf{x}_i\}_{i=0}^{\infty} \in \Phi \subset \mathbb{R}^2$. We assume that users (dual-antenna receivers) are independently distributed on the plane according to some stationary point process. By Slivnyak's Theorem [4], [5] and due to the stationarity of Φ, we can focus the analysis on a *typical* receiver/user located at the origin. All transmitted signals undergo a distance-dependent path loss of the form $\|\cdot\|^{-\alpha}$, where $\alpha > 2$ is the path loss exponent. We assume independent and identically distributed (i.i.d) frequency-flat slow Rayleigh fading on all links. The power fading gain between the i^{th} BS and the n^{th} antenna of the typical receiver is denoted by $\mathsf{h}_{n,i}$ following a unit-mean exponential distribution.

Users are assumed to associate with the BS providing the strongest average received power, i.e., with their closest BS. Without loss of generality, we let the 0^{th} BS be the closest one to the typical user and denote its distance $\|x_0\|$ by d. For notational convenience we define $\Phi_0 \triangleq \Phi \setminus \{x_0\}$, i.e., the set of locations of interfering BSs. Note that conditioned on $\mathsf{x}_0 = d$, Φ_0 is a homogeneous PPP on $\mathbb{R}^2 \setminus b(0, d)$. We consider the case of fixed transmit power across all BSs and assume that interference is treated as white noise. We denote by $\mathtt{SNR}$ the transmit-signal-to-noise ratio. The (transmit-power normalized) interference power experienced by the typical user at the n^{th} antenna can then be written as

$$\mathsf{I}_n \triangleq \sum_{\mathsf{x}_i \in \Phi_0} \mathsf{h}_{n,i} \|\mathsf{x}_i\|^{-\alpha}. \tag{1}$$

Receivers use MRC to coherently combine the signals received at the two antennas. We assume that they can perfectly estimate not only the instantaneous channel but also the current interference-plus-noise power at each antenna. Following [15], the MRC weight corresponding to the n^{th} antenna is then proportional to $\sqrt{\mathsf{h}_{n,0}}/(\mathsf{I}_n + \mathtt{SNR}^{-1})$. The post-combiner signal-to-interference-plus-noise ratio ($\mathtt{SINR}$) under MRC at the typical user then takes the form [11], [12]

$$\mathtt{SINR}_{\text{MRC}} \triangleq \frac{\mathsf{h}_{1,0}\mathsf{d}^{-\alpha}}{\mathsf{I}_1 + \mathtt{SNR}^{-1}} + \frac{\mathsf{h}_{2,0}\mathsf{d}^{-\alpha}}{\mathsf{I}_2 + \mathtt{SNR}^{-1}}. \tag{2}$$

Note that, although the fading gains $\mathsf{h}_{n,i}$ are mutually independent across n, i, the interference terms I_1 and I_2 are correlated due to the common locations of interferers.

III. Coverage Probability Analysis

In this section, we study the downlink performance of the typical dual-antenna MRC receiver.

Definition 1 (Coverage Probability $\mathtt{P}_{\text{c}}$)**.** *The coverage probability is the probability of the* $\mathtt{SINR}$ *exceeding a predefined coding-/modulation-specific threshold* $T > 0$*, i.e.,*

$$\mathtt{P}_{\text{c}} \triangleq \mathbb{P}\left(\mathtt{SINR} > T\right). \tag{3}$$

In the next subsection, we consider the setting described in Section II, which models the exact interference correlation.

A. Analysis with Exact Interference Correlation Model

The next result characterizes the typical downlink performance of dual-antenna MRC receivers in a cellular network.

Theorem 1 ($\mathtt{P}_{\text{c,MRC}}$ for Dual-Antenna MRC)**.** *The coverage probability for a typical dual-antenna MRC receiver is*

$$\mathtt{P}_{\text{c,MRC}} = -\int_0^{\infty} 2\pi\lambda d \int_0^{\infty} e^{-\frac{d^{\alpha}}{\mathtt{SNR}}(T-z)^+} \times \frac{\partial}{\partial w}\left[e^{-\frac{d^{\alpha}}{\mathtt{SNR}}w}\, e^{-\lambda\pi d^2 \mathcal{A}(z,w)}\right]_{w=z} \mathrm{d}z\, \mathrm{d}d, \tag{4}$$

where

$$\mathcal{A}(z,w) \triangleq \tfrac{(T-z)^+}{(T-z)^+ - w}\, {}_2F_1\big(1, -\tfrac{2}{\alpha}, 1-\tfrac{2}{\alpha}; -(T-z)^+\big) - \tfrac{w}{(T-z)^+ - w}\, {}_2F_1\big(1, -\tfrac{2}{\alpha}, 1-\tfrac{2}{\alpha}; -w\big) \tag{5}$$

and ${}_2F_1(a,b,c;z)$ *is the Gauss hypergeometric function [16].*

Proof: See Appendix A. ∎

For certain integer α, $\mathcal{A}(z,w)$ in (5) can be expressed through elementary function using identities of the Gauss hypergeometric function [16], e.g., ${}_2F_1\big(1, -\frac{1}{2}, \frac{1}{2}; -u\big) = 1 + \sqrt{u}\arctan\sqrt{u}$ for $\alpha = 4$. For general α, (4) can be easily evaluated using standard numerical softwares.

Well-designed dense cellular networks typically operate in the interference-limited regime ($\mathtt{SNR} \to \infty$). In this case, the effect of receiver noise can be ignored, thereby yielding a simplified expression for $\mathtt{P}_{\text{c,MRC}}$.

Corollary 1 (Interference-limited $\mathtt{P}_{\text{c,MRC}}$ for Dual-Antenna MRC)**.** *In the absence of noise* ($\mathtt{SNR} \to \infty$)*, the general expression in Theorem 1 reduces to*

$$\mathtt{P}_{\text{c,MRC}} = \frac{1}{{}_2F_1\big(1, -\frac{2}{\alpha}, 1-\frac{2}{\alpha}; -T\big)} + \mathcal{B}(\alpha, T), \tag{6}$$

where $\mathcal{B}(\alpha, T)$ *is defined in* (7) *at the top of the next page.*

Interestingly, the coverage probability is independent of the BS density λ, which is consistent with [17]. Fig. 1 shows the coverage probability $\mathtt{P}_{\text{c,MRC}}$ of (6) for different α. It can be

$$\mathcal{B}(\alpha,T) \triangleq \int_0^T \frac{2T-4z-(1+z)\left((T(2+\alpha)-z(4+\alpha))_2F_1\!\left(1,-\frac{2}{\alpha},1-\frac{2}{\alpha};-z\right)+\alpha(z-T)_2F_1\!\left(1,-\frac{2}{\alpha},1-\frac{2}{\alpha};-T+z\right)\right)}{\alpha(1+z)\left(z\,{}_2F_1\!\left(1,-\frac{2}{\alpha},1-\frac{2}{\alpha};-z\right)+(-T+z)\,{}_2F_1\!\left(1,-\frac{2}{\alpha},1-\frac{2}{\alpha};-T+z\right)\right)^2} \quad (7)$$

seen that the analysis perfectly matches the simulation results. Furthermore, $\mathsf{P}_{\mathrm{c,MRC}}$ monotonically increases with α as a result of reducing the impact of far interfering BSs.

Remark 1. *The first summand in* (6) *corresponds to the coverage probability for the single-antenna case. This, in turn, means that* $\mathcal{B}(\alpha,T)$ *in* (6) *fully characterizes the coverage probability gain of dual-antenna MRC in cellular networks.*

B. Comparison with Simpler Interference Correlation Models

In this section, we characterize the performance of MRC under two popular though simpler correlation models frequently used in the literature. Using the results from Section III-A, the validity of these models will be discussed in Section IV.

1) No-Correlation Model: A commonly made assumption to maintain analytical tractability is to assume that I_1 and I_2 are uncorrelated, i.e., the interferer locations in I_1 and I_2 originate from two separate independent point processes. Under this assumption, we next derive the corresponding coverage probability denoted by $\mathsf{P}_{\mathrm{c,MRC}}^{\mathrm{NC}}$.

Proposition 1 (Coverage Probability $\mathsf{P}_{\mathrm{c,MRC}}^{\mathrm{NC}}$)**.** *The coverage probability for a typical dual-antenna MRC receiver in the no-correlation model is*

$$\mathsf{P}_{\mathrm{c,MRC}}^{\mathrm{NC}} = -\int_0^\infty 2\pi\lambda d\, e^{\pi\lambda d^2} \int_0^\infty e^{-\frac{d^\alpha}{\mathtt{SNR}}(T-z)^+} \times e^{-\pi\lambda d^2 {}_2F_1\left(1,-\frac{2}{\alpha},1-\frac{2}{\alpha};-(T-z)^+\right)} \times \frac{\partial}{\partial w}\Big[e^{-\frac{d^\alpha}{\mathtt{SNR}}w} e^{-\lambda\pi d^2 {}_2F_1\left(1,-\frac{2}{\alpha},1-\frac{2}{\alpha};-w\right)}\Big]_{w=z} \mathrm{d}z\,\mathrm{d}d. \quad (8)$$

Proof: See Appendix B. ∎

By comparing the mathematical form of the inner integrals in (8) and (4), the influence of correlated interference becomes apparent: While in (8) the inner integral reduces to the well-known convolution formula for sums of two independent random variables [18], this is not the case in (4) since $\mathcal{A}(z,w)$ cannot be further simplified to a similar convolution form.

2) Full-Correlation Model: Another technique used in the literature to simplify the analysis is to assume that I_1 and I_2 are fully correlated, i.e., the fading gains $\mathsf{h}_{1,i}$ and $\mathsf{h}_{2,i}$ are no longer independent and yield the same realizations for all $i \in \mathbb{N}_{>0}$. Under this assumption, the corresponding coverage probability $\mathsf{P}_{\mathrm{c,MRC}}^{\mathrm{FC}}$ can be derived for an arbitrary number of antennas as shown next.

Proposition 2 (Coverage Probability $\mathsf{P}_{\mathrm{c,MRC}}^{\mathrm{FC}}$)**.** *The coverage probability for a typical N-antenna MRC receiver in the full-correlation model is*

$$\mathsf{P}_{\mathrm{c,MRC}}^{\mathrm{FC}} = \sum_{n=0}^{N-1} \frac{(-1)^n}{n!} \int_0^\infty 2\pi\lambda d\, \frac{\partial^n}{\partial s^n}\Big[e^{-\frac{d^\alpha}{\mathtt{SNR}}sT} \times e^{-\lambda\pi d^2 {}_2F_1\left(1,-\frac{2}{\alpha},1-\frac{2}{\alpha};-sT\right)}\Big]_{s=1} \mathrm{d}d. \quad (9)$$

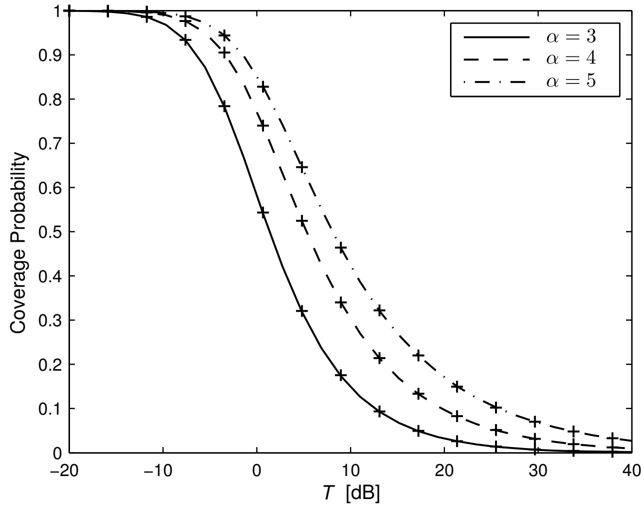

Fig. 1. Coverage probability for different path loss exponents α. Marks represent simulation results.

Proof: See Appendix C. ∎

Without receiver noise ($\mathtt{SNR} \to \infty$), (9) simplifies to

$$\mathsf{P}_{\mathrm{c,MRC}}^{\mathrm{FC}} = \sum_{n=0}^{N-1} \frac{(-1)^n}{n!} \frac{\partial^n}{\partial s^n}\left[\frac{1}{{}_2F_1\left(1,-\frac{2}{\alpha},1-\frac{2}{\alpha};-sT\right)}\right]_{s=1}. \quad (10)$$

C. Comparison with Selection Combining

Strict complexity constraints of mobile devices may sometimes prevent the use of MRC, allowing only for combining schemes with low complexity. One such wide-spread technique is SC, in which the antenna providing the highest instantaneous $\mathtt{SINR}$ among all others is chosen. Unlike in the noise-limited scenario, the relative performance between MRC and SC under spatially-correlated interference is not well understood. For interference-limited decentralized networks, the performance of MRC and SC under spatially-correlated interference was recently compared in [11]. We next extend this comparison to the cellular network case.

Theorem 2 (SC Coverage Probability $\mathsf{P}_{\mathrm{c,SC}}$)**.** *The coverage probability for a typical N-antenna SC receiver is*

$$\mathsf{P}_{\mathrm{c,SC}} = \sum_{n=1}^{N} (-1)^n \binom{N}{n} \int_0^\infty 2\lambda\pi d\, e^{-\frac{d^\alpha T}{\mathtt{SNR}}n} \times \exp\Bigg\{-\lambda\pi d^2\Big(\frac{T^{2/\alpha}}{\Gamma(n)}\Gamma\left(1-\tfrac{2}{\alpha}\right)\Gamma\left(n+\tfrac{2}{\alpha}\right) + \frac{\frac{2}{\alpha}T^{-n}}{n+\frac{2}{\alpha}} {}_2F_1\left(n, n+\tfrac{2}{\alpha}, n+\tfrac{2}{\alpha}+1; -\tfrac{1}{T}\right)\Big)\Bigg\}. \quad (11)$$

Proof: Due to space limitations, we present a proof sketch. We follow the same procedure as in the proof of

Theorem 1 in [6] to obtain the joint success probability at N antennas for a fixed d. Here, we exploit the fact that the term related to the receiver noise can be moved outside the Φ_0-expectation. After computing the joint success probability, we invoke [6, Eq. (8)] and finally average over d. ■

When receiver noise can be ignored, the expression in (11) reduces to

$$\lim_{\mathtt{SNR}\to\infty} \mathrm{P}_{\mathrm{c,SC}} = \sum_{n=1}^{N} (-1)^n \binom{N}{n} \left(\frac{T^{2/\alpha}}{\Gamma(n)} \Gamma\left(1 - \frac{2}{\alpha}\right) \Gamma\left(n + \frac{2}{\alpha}\right) + \frac{\frac{2}{\alpha} T^{-n}}{n + \frac{2}{\alpha}} {}_2F_1\left(n, n + \frac{2}{\alpha}, n + \frac{2}{\alpha} + 1; -\frac{1}{T}\right)\right)^{-1}. \quad (12)$$

IV. Modeling and Design Insights

Due to limited space, the next discussions will be restricted to the interference-limited case ($\mathtt{SNR} \to \infty$), which applies to dense cellular networks. Discussing the joint impact of receiver noise and interference is left for possible future work.

We first analyze the gain of dual-branch MRC over single-antenna receivers in terms of relative coverage probability increase. Using Remark 1, the relative increase can readily be obtained as $\mathcal{B}(\alpha, T)/{}_2F_1\big(1, -\frac{2}{\alpha}, 1 - \frac{2}{\alpha}; -T\big)$. Fig. 2 shows the relative coverage probability increase over the path loss α and the $\mathtt{SINR}$ threshold T. The improvement obtained by MRC is maximal for small α and monotonically decreases with α. This is because, for smaller α, the interference is no longer dominated by a few nearby BSs but by many—possibly far—BSs. Consequently, the set of effective interferers becomes large, which, in turn reduces the correlation across the antennas, and hence improves the performance of MRC. Interestingly, the coverage probability improvement converges to a non-zero constant as T increases, although in the interference-free case the improvement (measured in 1-outage probability) is known to tend to zero [19, 7.2.4]. For typical operating points ($3 < \alpha < 5$ and $T > -6\,\mathrm{dB}$), the improvement obtained by MRC is between 12%–67%.

Figure 3 shows the coverage probability gap for the two simpler correlation models for different α. The gap is defined as $\delta \triangleq \mathrm{P}^{\mathrm{NC}}_{\mathrm{c,MRC}}/\mathrm{P}_{\mathrm{c,MRC}} - 1$ ($\delta \triangleq \mathrm{P}^{\mathrm{FC}}_{\mathrm{c,MRC}}/\mathrm{P}_{\mathrm{c,MRC}} - 1$) for the respective correlation model. First, it can be seen that both models reflect the true performance at small T, i.e., at small target spectral efficiencies. For $T > 0$ dB, the no-correlation model yields a significantly optimistic performance prediction (coverage probability gap is 3%–10%), depending on α. In contrast, the full-correlation model slightly underestimates the true performance (P_c gap $< 2\%$). The smaller gap of the full-correlation model was already reported in [12] and is reconfirmed in this work for the cellular network case.

Figure 4 illustrates the outage probability (1-coverage probability) for the exact, no-correlation and full-correlation models for different α. It can be seen that the simpler correlation models preserve the true diversity order for dual-antenna MRC. Interestingly, the diversity order (which is equal to two) remains unaffected by the fact that interference is correlated across antennas. This is in contrast to the diversity analysis for decentralized networks, where interferers may be closer than the desired transmitter [11].

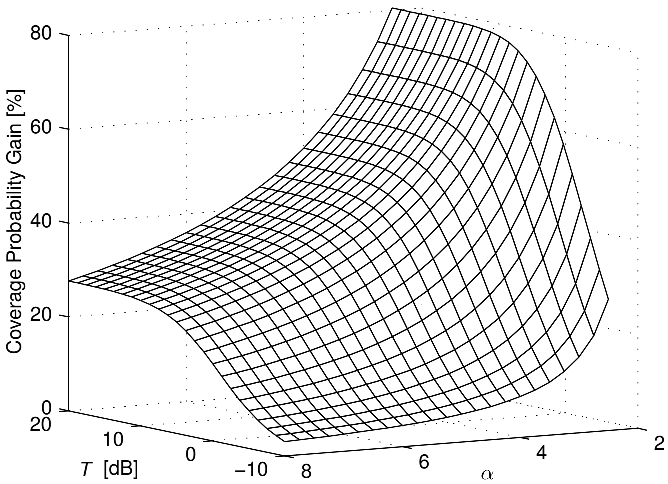

Fig. 2. Coverage probability gain of dual-antenna MRC over single-antenna receivers for different T and α.

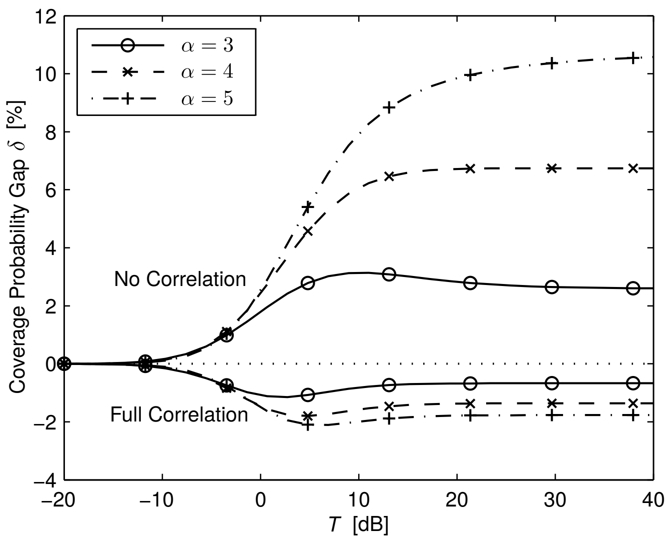

Fig. 3. Coverage probability gap of no-correlation and full-correlation model for different path loss exponents α.

Figure 5 shows the relative P_c gain of MRC over SC for the three interference models and for different α. In accordance with [12], the superiority of MRC increases as α becomes small, i.e., when interference is more severe. For $\alpha = 3$, the gains are between 10%–20%, while for $\alpha = 5$ the gains are between 5%–11% for practically relevant T (e.g., $T > -5$ dB for LTE). We thus conclude that for large path loss exponents and low target spectral efficiencies, the higher complexity of MRC might not be justified as SC achieves comparable performance. It can also be observed that, depending on α, the much simpler interference correlation models result in a considerably distorted performance comparison for practically relevant T. In particular, the no-correlation model significantly overestimates the gain of MRC over SC at high path loss exponents (by a factor of two at $\alpha = 5$ and $T = 12$ dB).

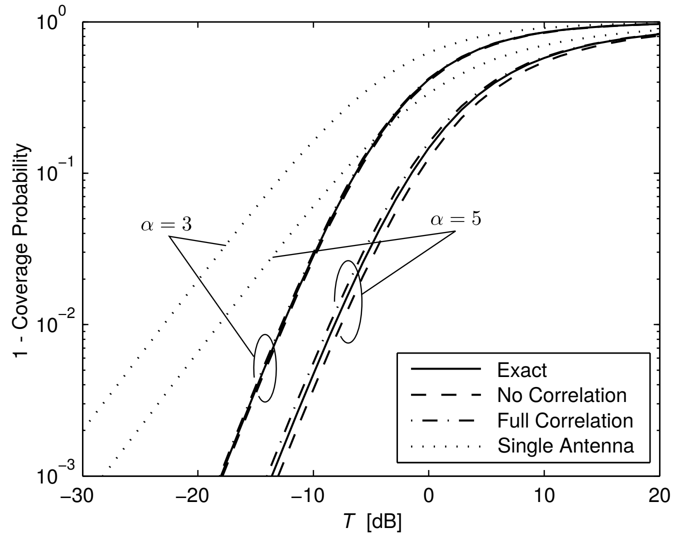

Fig. 4. Outage probability comparison between exact correlation, no-correlation and full-correlation models for different α. Results for the single-antenna case are also shown for reference.

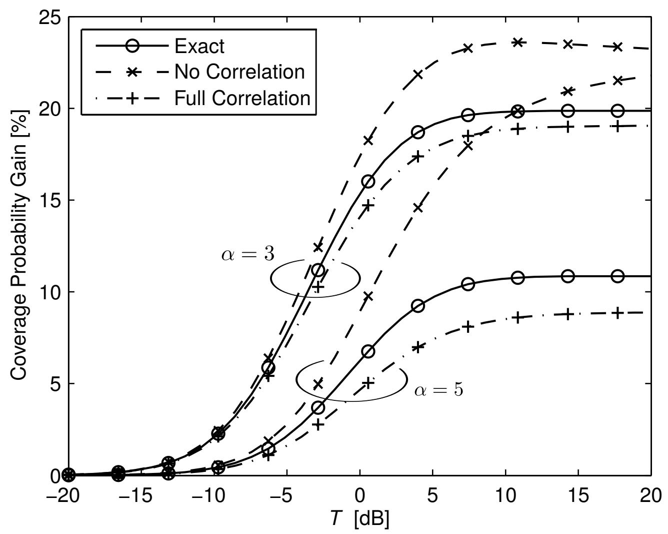

Fig. 5. Coverage probability gain of dual-branch MRC over dual-branch SC for the different correlation models.

V. Conclusion

We presented an analytical framework for analyzing the impact of spatial interference correlation on the downlink performance of dual-antenna MRC receivers in a cellular network. Using tools from stochastic geometry, we derived the coverage probability for a typical dual-branch MRC receiver. Using the theoretical results, we discussed related modeling and design aspects of potential importance to designers of commercial diversity-combining techniques. Future work may include an extension to the case of more than two antennas at the MRC receiver and multiple antennas at the base stations. Another useful direction of future work is to evaluate the downlink rate achievable per user accounting for the load on each base station.

Appendix

A. Proof of Theorem 1

Conditioning (2) on a fixed distance d to the serving BS yields

$$\mathtt{P}_{\text{c,MRC}}(d) = \mathbb{P}\left(\frac{\mathsf{h}_{1,0}d^{-\alpha}}{\mathsf{I}_1 + \mathtt{SNR}^{-1}} + \frac{\mathsf{h}_{2,0}d^{-\alpha}}{\mathsf{I}_2 + \mathtt{SNR}^{-1}} \geq T\right). \quad (13)$$

The probability in (13) for a given link distance d was recently derived in [12] and can be written as [12, Eq. (35)]

$$\mathtt{P}_{\text{c,MRC}}(d) = -\int_0^\infty e^{-\frac{d^\alpha}{\mathtt{SNR}}(T-z)^+}\frac{\partial}{\partial w}\Bigg[e^{-\frac{d^\alpha}{\mathtt{SNR}}w} \times \mathbb{E}_{\Phi_0}\Bigg[\prod_{\mathsf{x}_i\in\Phi_0}\mathbb{E}_{\mathsf{h}_{1,i},\mathsf{h}_{2,i}}\Big[e^{-d^\alpha\|\mathsf{x}_i\|^{-\alpha}\left((T-z)^+\mathsf{h}_{1,i}+w\mathsf{h}_{2,i}\right)}\Big]\Bigg]\Bigg]_{w=z}\mathrm{d}z, \quad (14)$$

where we have exploited the independent-fading property. Since $\mathsf{h}_{1,i}$ and $\mathsf{h}_{2,i}$ follow a unit-mean exponential distribution for all $i \in \mathbb{N}_0$, the expectation with respect to the fading gains can be computed as

$$\begin{aligned}&\mathbb{E}_{\mathsf{h}_{1,i},\mathsf{h}_{2,i}}\left[e^{-d^\alpha\|\mathsf{x}_i\|^{-\alpha}\left((T-z)^+\mathsf{h}_{1,i}+w\mathsf{h}_{2,i}\right)}\right]\\ &\quad= \mathbb{E}_{\mathsf{h}_{1,i}}\left[e^{-d^\alpha\|\mathsf{x}_i\|^{-\alpha}(T-z)^+\mathsf{h}_{1,i}}\right]\times\mathbb{E}_{\mathsf{h}_{2,i}}\left[e^{-d^\alpha\|\mathsf{x}_i\|^{-\alpha}w\mathsf{h}_{2,i}}\right]\\ &\quad\overset{\text{(a)}}{=}\frac{1}{1+d^\alpha\|\mathsf{x}_i\|^{-\alpha}(T-z)^+}\frac{1}{1+d^\alpha\|\mathsf{x}_i\|^{-\alpha}w},\end{aligned} \quad (15)$$

where (a) follows from the Laplace transform for exponential random variables [18]. Inserting (15) back into (14) and invoking the probability generating functional (PGFL) $\mathbb{E}\left[\prod_{\mathsf{x}_i\in\Phi\cap A}1-\Delta(\mathsf{x}_i)\right] = \exp(-\lambda\int_A\Delta(x)\,\mathrm{d}x)$ for homogeneous PPPs [4], [5], the outer expectation over Φ yields

$$\exp\Bigg\{-\lambda\pi\int_d^\infty 2r\underbrace{\left(1-\frac{1}{1+d^\alpha r^{-\alpha}(T-z)^+}\times\frac{1}{1+d^\alpha r^{-\alpha}w}\right)}_{\triangleq\ \xi(r)}\mathrm{d}r\Bigg\}. \quad (16)$$

To evaluate the integral in (16), we apply a partial fraction decomposition to $\xi(r)$ and obtain

$$\xi(r) = 1 - \frac{\frac{(T-z)^+}{(T-z)^+-w}}{1+d^\alpha r^{-\alpha}(T-z)^+} + \frac{\frac{w}{(T-z)^+-w}}{1+d^\alpha r^{-\alpha}w}. \quad (17)$$

Inserting (17) into (16) and using the substitution $t = d^\alpha r^{-\alpha}$, we get, after carefully evaluating the integral,

$$\begin{aligned}&\mathbb{E}_{\Phi_0}\left[\prod_{\mathsf{x}_i\in\Phi_0}\mathbb{E}_{\mathsf{h}_{1,i},\mathsf{h}_{2,i}}\left[e^{-d^\alpha\|\mathsf{x}_i\|^{-\alpha}\left((T-z)^+\mathsf{h}_{1,i}+w\mathsf{h}_{2,i}\right)}\right]\right]\\ &\quad=\exp\Big\{-\lambda\pi d^2\Big(\tfrac{(T-z)^+}{(T-z)^+-w}{}_2F_1\big(1,-\tfrac{2}{\alpha},1-\tfrac{2}{\alpha};-(T-z)^+\big)\\ &\qquad-\tfrac{w}{(T-z)^+-w}{}_2F_1\big(1,-\tfrac{2}{\alpha},1-\tfrac{2}{\alpha};-w\big)-1\Big)\Big\}.\end{aligned} \quad (18)$$

Substituting (18) back into (14), we obtain a single-integral expression for the conditional probability $\mathtt{P}_{\text{c,MRC}}(d)$. To obtain the final result, $\mathtt{P}_{\text{c,MRC}}(d)$ needs to be averaged over d, which has a Rayleigh probability density function $f_{\mathsf{d}}(d) = 2\lambda\pi d e^{-\lambda\pi d^2}$ [5]. The result then follows by observing that the $e^{-\lambda\pi d^2}$ term from $f_{\mathsf{d}}(d)$ and the last summand in the exp-term of (18) cancel each other. ■

B. Proof of Proposition 1

Recall that in the no-correlation model the interferer locations originate from different point processes, say Φ_0 and Φ_0', for each of the two antennas. Hence, we can rewrite (14) as

$$\mathsf{P}_{\text{c,MRC}}^{\text{NC}}(d) = -\int_0^\infty e^{-\frac{d^\alpha}{\mathtt{SNR}}(T-z)^+} \times \mathbb{E}_{\Phi_0}\left[\prod_{\mathsf{x}_i\in\Phi_0}\mathbb{E}_{\mathsf{h}_{1,i}}\left[e^{-d^\alpha\|\mathsf{x}_i\|^{-\alpha}(T-z)^+\mathsf{h}_{1,i}}\right]\right] \times \frac{\partial}{\partial w}\left[e^{-\frac{d^\alpha}{\mathtt{SNR}}w}\,\mathbb{E}_{\Phi_0'}\left[\prod_{\mathsf{x}_i\in\Phi_0'}\mathbb{E}_{\mathsf{h}_{2,i}}\left[e^{-d^\alpha\|\mathsf{x}_i\|^{-\alpha}w\mathsf{h}_{2,i}}\right]\right]\right]_{w=z}\mathrm{d}z, \tag{19}$$

Again invoking the PGFL for PPPs and the Laplace transform for exponential random variables, the expectation over Φ_0 yields,

$$\begin{aligned}&\mathbb{E}_{\Phi_0}\left[\prod_{\mathsf{x}_i\in\Phi_0}\mathbb{E}_{\mathsf{h}_{1,i}}\left[e^{-d^\alpha\|\mathsf{x}_i\|^{-\alpha}(T-z)^+\mathsf{h}_{1,i}}\right]\right]\\ &= \exp\left\{-\lambda\pi\int_d^\infty 2r\left(1-\frac{1}{1+d^\alpha r^{-\alpha}(T-z)^+}\right)\mathrm{d}r\right\}\\ &= \exp\left\{-\lambda\pi d^2\left({}_2F_1\big(1,-\tfrac{2}{\alpha},1-\tfrac{2}{\alpha};-(T-z)^+\big)-1\right)\right\}.\end{aligned} \tag{20}$$

Analogously, the expectation over Φ_0' can be computed as $\exp\{-\lambda\pi d^2\left({}_2F_1\big(1,-\frac{2}{\alpha},1-\frac{2}{\alpha};-w\big)-1\right)\}$. Averaging over the distance d yields the final result. ■

C. Proof of Proposition 2

The full-correlation model requires the interference terms at the N antennas to be equally-strong, i.e., $\mathsf{I}_1 \equiv \ldots \equiv \mathsf{I}_N$. The $\mathtt{SINR}$ then takes the form

$$\mathtt{SINR}_{\text{FC}} = \frac{\mathsf{d}^{-\alpha}\sum_{n=1}^N \mathsf{h}_{n,0}}{\mathsf{I}_1 + \mathtt{SNR}^{-1}}, \tag{21}$$

where $\sum_{n=1}^N \mathsf{h}_{n,0}$ follows a chi-square distribution with $2N$ degrees of freedom [19]. Hence, the coverage probability conditional on $\mathsf{d} = d$ can be written as

$$\begin{aligned}\mathsf{P}_{\text{c,MRC}}^{\text{FC}}(d) &= \mathbb{P}\left(\sum_{n=1}^N \mathsf{h}_{n,0} \geq d^\alpha T\left(\mathsf{I}_1+\mathtt{SNR}^{-1}\right)\right)\\ &\overset{\text{(a)}}{=} \mathbb{E}\left[\sum_{n=0}^{N-1}\frac{1}{n!}\left(d^\alpha T\left(\mathsf{I}_1+\mathtt{SNR}^{-1}\right)\right)^n e^{-d^\alpha T\left(\mathsf{I}_1+\mathtt{SNR}^{-1}\right)}\right]\\ &\overset{\text{(b)}}{=} \sum_{n=0}^{N-1}\frac{1}{n!}\mathbb{E}\left[\left(d^\alpha T\left(\mathsf{I}_1+\mathtt{SNR}^{-1}\right)\right)^n e^{-d^\alpha T\left(\mathsf{I}_1+\mathtt{SNR}^{-1}\right)}\right]\\ &\overset{\text{(c)}}{=} \sum_{n=0}^{N-1}\frac{(-1)^n}{n!}\frac{\partial^n}{\partial s^n}\left[\mathcal{L}_{d^\alpha T(\mathsf{I}_1+\mathtt{SNR}^{-1})}(s)\right]_{s=1},\end{aligned} \tag{22}$$

where (a) follows from conditioning on I_1 and evaluating the probability with respect to $\sum_{n=1}^N \mathsf{h}_{n,0}$, (b) is a consequence of the linearity of the expectation and (c) follows from the differentiation correspondence for Laplace transforms [18]. The Laplace transform $\mathcal{L}_{d^\alpha T(\mathsf{I}_1+\mathtt{SNR}^{-1})}(s)$ is obtained as

$$\begin{aligned}&\mathcal{L}_{d^\alpha T(\mathsf{I}_1+\mathtt{SNR}^{-1})}(s)\\ &= e^{-\frac{d^\alpha}{\mathtt{SNR}}sT}\,\mathbb{E}\left[e^{-sd^\alpha T\mathsf{I}_1}\right]\\ &= e^{-\frac{d^\alpha}{\mathtt{SNR}}sT}\,\mathbb{E}_{\Phi_0}\left[\prod_{\mathsf{x}_i\in\Phi_0}\mathbb{E}_{\mathsf{h}_{1,i}}\left[e^{-sd^\alpha T\mathsf{h}_{1,i}\|\mathsf{x}_i\|^{-\alpha}}\right]\right]\\ &\overset{(20)}{=} e^{-\frac{d^\alpha}{\mathtt{SNR}}sT}e^{-\lambda\pi d^2\left({}_2F_1\left(1,-\frac{2}{\alpha},1-\frac{2}{\alpha};-sT\right)-1\right)}.\end{aligned} \tag{23}$$

Substituting (23) back into (22) and averaging over d yields the final result. ■

References

[1] S. Halpern, "The effect of having unequal branch gains practical predetection diversity systems for mobile radio," *IEEE Trans. Veh. Technol.*, vol. 26, no. 1, pp. 94–105, Feb. 1977.

[2] V. Aalo, "Performance of maximal-ratio diversity systems in a correlated Nakagami-fading environment," *IEEE Trans. Commun.*, vol. 43, no. 8, pp. 2360–2369, Aug. 1995.

[3] X. Cui, Q. Zhang, and Z. Feng, "Outage performance for maximal ratio combiner in the presence of unequal-power co-channel interferers," *IEEE Commun. Lett.*, vol. 8, no. 5, pp. 289–291, May 2004.

[4] D. Stoyan, W. Kendall, and J. Mecke, *Stochastic Geometry and its Applications*, 2nd ed. Wiley, 1995.

[5] M. Haenggi, *Stochastic Geometry for Wireless Networks*. Cambridge University Publishers, 2012.

[6] ——, "Diversity Loss due to Interference Correlation," *IEEE Commun. Lett.*, vol. 16, no. 10, pp. 1600–1603, Oct. 2012.

[7] A. Chopra, "Modeling and mitigation of interference in wireless receivers with multiple antennae," Ph.D. dissertation, The University of Texas at Austin, Dec. 2011.

[8] A. Chopra and B. Evans, "Joint statistics of radio frequency interference in multiantenna receivers," *IEEE Trans. Signal Process.*, vol. 60, no. 7, pp. 3588–3603, Jul. 2012.

[9] R. Tanbourgi, H. Jäkel, and F. K. Jondral, "Cooperative relaying in a Poisson field of interferers: A diversity order analysis," in *IEEE Int. Symposium on Inf. Theory (ISIT)*, Istanbul, Turkey, Jul. 2013.

[10] M. Haenggi and R. Smarandache, "Diversity polynomials for the analysis of temporal correlations in wireless networks," *IEEE Trans. Wireless Commun.*, vol. 12, no. 11, pp. 5940–5951, Nov. 2013.

[11] R. Tanbourgi, H. S. Dhillon, J. G. Andrews, and F. K. Jondral, "Effect of spatial interference correlation on the performance of maximum ratio combining," 2014, to appear in *IEEE Trans. Wireless Commun.*, available online: http://arxiv.org/abs/1307.6373.

[12] ——, "Dual-branch MRC receivers under spatial interference correlation and Nakagami fading," Dec. 2013, under revision for *IEEE Trans. Commun.*, available online: http://arxiv.org/abs/1312.5938.

[13] A. Rajan and C. Tepedelenlioglu, "Diversity combining over Rayleigh fading channels with symmetric alpha-stable noise," *IEEE Trans. Wireless Commun.*, vol. 9, no. 9, pp. 2968–2976, Sep. 2010.

[14] A. M. Hunter, J. G. Andrews, and S. Weber, "Transmission capacity of ad hoc networks with spatial diversity," *IEEE Trans. Wireless Commun.*, vol. 7, no. 12, pp. 5058–5071, Dec. 2008.

[15] D. G. Brennan, "Linear diversity combining techniques," *Proc. IEEE*, vol. 91, no. 2, pp. 331–356, Feb. 2003.

[16] F. W. Olver, D. W. Lozier, R. F. Boisvert, and C. W. Clark, *NIST Handbook of Mathematical Functions*, 1st ed. New York, NY, USA: Cambridge University Press, 2010.

[17] J. G. Andrews, F. Baccelli, and R. K. Ganti, "A tractable approach to coverage and rate in cellular networks," *IEEE Trans. Commun.*, vol. 59, no. 11, pp. 3122 –3134, Nov. 2011.

[18] W. Feller, *An Introduction to Probability Theory and Its Applications, Vol. 2*, 2nd ed. Wiley, Jan 1971.

[19] A. Goldsmith, *Wireless Communications*. Cambridge, New York: Cambridge University Press, 2005.